Electrically tunable Dirac-point resonance induced by a nanomagnet absorbed on the topological insulator surface

Rui-Qiang Wang,[1] L. Sheng,[2] M. Yang,[1] Baigeng Wang,[2] and D. Y. Xing[2]

[1]*Laboratory of Quantum Engineering and Quantum Materials, ICMP and SPTE, South China Normal University, Guangzhou 510006, China*

[2]*National Laboratory of Solid State Microstructures, School of Physics, and Collaborative Innovation Center of Advanced Microstructures, Nanjing University, Nanjing 210093, China*

(Received 20 January 2015; revised manuscript received 7 May 2015; published 9 June 2015)

We investigate the effect of spin-inelastic scattering of Dirac electrons off a high-spin nanomagnet adsorbed on a topological insulator (TI) surface, in which transitions of the nanomagnet between its internal magnetic levels are taken into account, beyond the classic spin theory. It is found that the presence of magnetic anisotropy of nanomagnets can result in a Dirac-point resonance peak in local density of states. It can significantly modify the topologically protected Dirac surface-state spectrum at the Dirac point, quite different from previously reported low-energy resonances. Furthermore, we propose to tune electrically the appearance of the Dirac-point resonance peak and its height by use of the spin-flip torque effect. This provides an approach to engineer the Dirac cone and tune the Dirac electron properties on the TI surface in the absence of an external magnetic field.

DOI: 10.1103/PhysRevB.91.245409 PACS number(s): 72.25.−b, 73.20.−r, 75.30.Hx, 85.75.−d

I. INTRODUCTION

Topological insulators (TIs), a new class of topologically nontrivial states of matter, are currently attracting great interest in condensed-matter physics due to their promising applications for spintronics and topological quantum computation. In a three-dimensional TI, the topological structure of the gapped bulk energy bands gives rise to gapless surface states with Dirac linear dispersion and helical spin texture, which is quite different from those in a single-layer graphene. The helical spin texture prohibits backscattering of surface electrons from any time-reversal invariant perturbation and protects the Dirac dispersion [1,2]. Applications of topological surface states (TSSs) require the manipulation of the Dirac electronic properties or engineering Dirac cones [3].

A tremendous effort has been devoted to the robustness of the TSSs against magnetic impurities [4–14], but currently there is no consensus on the behavior of magnetic impurities in experimental and theoretical literatures. For instance, some works [4–8] reported that magnetic doping can destroy the Dirac point of the TSSs by opening a local gap while some others [9–14] demonstrated that the Dirac node remains immune from magnetic perturbations. More interesting is the tunneling spectrum measurement for Fe atoms with magnetic anisotropy absorbed on Bi_2Te_3 materials [10,15], where an energy gap was not observed at the Dirac point, and instead a considerably strong resonance was found nearby. Theoretically, similar resonances were also predicted in scattering of the TSSs either by strong impurity potential [9,16] or by local bosons [17]. Note that although these resonances significantly modify the local density of states (LDOS) near the Dirac node they do not destroy the Dirac point for absorbed magnetic or nonmagnetic impurities.

Expectedly, magnetic impurities should exhibit a different way to affect the LDOS of the Dirac point since they can break time-reversal symmetry and allow spin-flip scattering. We note that most theoretical studies were based on a simple model of classic magnetic impurities with fixed magnetization. However, a magnetic impurity usually exhibits quantum behavior and spin dynamics, and so should be treated as quantum entities [18–22]. One of the remarkable merits of the quantum impurity model can be seen by considering the effect of internal degrees of freedom of impurities, such as magnetic excitations and localized vibrational modes. During the scattering processes of the surface electrons, by exchanging spin angular momentum or energy, the internal excitations can profoundly modify the low-energy TSSs, even resulting in interesting inelastic Friedel oscillations [17,23,24].

In this paper, we extend the classic spin model by considering quantum scattering processes involving transitions between its internal magnetic levels, and investigate the spin-inelastic scattering of Dirac electrons off a high-spin nanomagnet with magnetic anisotropy [25–27], adsorbed on a TI surface. It is found that introduction of the nanomagnet creates significant low-energy resonance peaks of LDOS, either located exactly at or near the Dirac point, depending on the strength of magnetic anisotropy. The former is especially interesting because it can locally modify the electronic spectrum at the Dirac point, quite different from the latter, which always remains the vanished LDOS at the Dirac point. In our theory, the formation of Dirac-point resonance (DPR) requires moderately strong anisotropy to enhance the spin-inelastic transitions. Experimentally, the requirement is difficult to meet and thus we further propose to tune electrically the appearance of DPR and its height by the spin-flip torque effect in a spin-polarized scanning tunneling microscope (STM).

II. MODEL AND THEORY

Consider a high-spin quantum nanomagnet **S**, e.g., a magnetic atom Fe or a single molecule magnet Mn_{12}, placed on a TI surface. The key features of the nanomagnet are captured by the spin Hamiltonian $H_{\rm spin} = -DS_z^2 - E(S_x^2 - S_y^2)$, where D and E define the uniaxial and in-plane magnetic anisotropy, respectively. The corresponding eigenvalues E_M and eigenstates $|M\rangle$ can be obtained by diagonalizing $H_{\rm spin}$ numerically in the space spanned by eigenstates of S_z. The TI surface is

described by the low-energy Dirac-type Hamiltonian:

$$H_{\rm TI} = \hbar v_F \sum_{\mathbf{k}} c^\dagger_{s\mathbf{k}}(k_x\sigma_y - k_y\sigma_x)c_{s\mathbf{k}}, \quad (1)$$

where $c^\dagger_{s\mathbf{k}} = (c^\dagger_{s\mathbf{k}\uparrow}, c^\dagger_{s\mathbf{k}\downarrow})$ is the creation operator of electrons with wave vector $\mathbf{k} = (k_x, k_y)$, σ denotes the vector of Pauli matrices in spin space, and v_F is the Fermi velocity. The conducting electrons on the TI surface are locally spin exchanged with the nanomagnet $\mathbf{S}$ via [28,29]

$$H^{\rm ex}_{ss} = \sum_{\mathbf{k}\mathbf{k}'} \frac{J_{ss}}{2} c^\dagger_{s\mathbf{k}}(\sigma_z S_z + \sigma_+ S_- + \sigma_- S_+)c_{s\mathbf{k}'}, \quad (2)$$

with $S_\pm = \frac{1}{2}(S_x \pm iS_y)$ and J_{ss} characterizing the exchange-coupling strength. This describes essentially deep cotunneling, in which the orbit levels are out of resonance with the Fermi level and the sequential tunneling is exponentially suppressed. Different from the classic spin, the quantum spin is defined as operators [30]

$$S^i(t) = \sum_{MM'} S^i_{MM'} d^\dagger_M(t) d_{M'}(t), (i = x,y,z), \quad (3)$$

where $S^i_{MM'} = \langle M|S^i|M'\rangle$ and $d^\dagger_M$ is the pseudofermion creation operator in magnetic level E_M.

By using the unitary transformation $U(\theta_{\mathbf{k}}) = \frac{1}{\sqrt{2}}\begin{pmatrix} 1 & ie^{-i\theta_{\mathbf{k}}} \\ ie^{i\theta_{\mathbf{k}}} & 1 \end{pmatrix}$ to diagonalize Eq. (1), where $\theta_{\mathbf{k}}$ is the azimuthal angle of momentum $\mathbf{k} = ke^{i\theta_{\mathbf{k}}}$, one obtains $H_{\rm TI} = \Sigma_{\mathbf{k}\sigma}\varepsilon_{\mathbf{k}\sigma}\gamma^\dagger_{s\mathbf{k},\sigma}\gamma_{s\mathbf{k},\sigma}$, where $\gamma_{s\mathbf{k}} = U^\dagger(\theta_{\mathbf{k}})c_{s\mathbf{k}}$ is the helical-state operator, and $\varepsilon_{\mathbf{k}\uparrow(\downarrow)} = \pm\varepsilon_{\mathbf{k}}$ with $\varepsilon_{\mathbf{k}} = \hbar v_F k$ represent the positive and negative energy branches, respectively. On the basis of the helical states, $H^{\rm ex}_{ss}$ is given by

$$\begin{aligned} H^{\rm ex}_{ss} &= \sum_{\mathbf{k}\mathbf{k}'} \frac{J_{ss}}{2}\gamma^\dagger_{s\mathbf{k}}[U^\dagger(\theta_{\mathbf{k}})\sigma U(\theta_{\mathbf{k}'})]\cdot\mathbf{S}\gamma_{s\mathbf{k}'} \\ &= \sum_{\mathbf{k}\mathbf{k}'} \frac{J_{ss}}{2}\gamma^\dagger_{s\mathbf{k}}[\sigma + \mathbf{h}(\theta_{\mathbf{k}},\theta_{\mathbf{k}'})]\cdot\mathbf{S}\gamma_{s\mathbf{k}'}. \end{aligned} \quad (4)$$

Here $\mathbf{h}(\theta_{\mathbf{k}},\theta_{\mathbf{k}'})$ is a matrix whose elements all consist of factor $e^{i\theta_{\mathbf{k}}}$ or $e^{i\theta_{\mathbf{k}'}}$, and the integration over the angle will vanish [31].

To study the multiple scattering of Dirac electrons off the quantum magnet, the T-matrix method is employed to calculate the real-space Green's function of the surface electrons [17,31,32]:

$$G(\mathbf{r},\mathbf{r}',i\omega) = G^0(\mathbf{r},\mathbf{r}',i\omega) + G^0(\mathbf{r},i\omega)T(i\omega)G^0(\mathbf{r}',i\omega), \quad (5)$$

where $G^0(\mathbf{r},i\omega) = \int G^0(\mathbf{k},i\omega)e^{i\mathbf{k}\cdot\mathbf{r}}d\mathbf{k}/(2\pi)^2$ is the bare Green's function with $G^0(\mathbf{k},i\omega) = 1/[i\omega - \hbar v_F(k_x\sigma_y - k_y\sigma_x)]$, and the T matrix is determined by the Bethe-Scalpeter equation $T(i\omega) = [1 - V_{im}(i\omega)G^0(0,i\omega)]^{-1}V_{im}(i\omega)$. The scattering potential is given by $V_{im}(i\omega) = \frac{J_{ss}}{2}\langle S_z\rangle\sigma_z + \Sigma(i\omega)$, the former describing the spin-conserving elastic scattering and the latter being the spin-flip inelastic scattering. Here $\langle S_z\rangle = \Sigma_M P_M\langle M|S_z|M\rangle$ is the average magnetization, $P_M = \langle d^\dagger_M d_M\rangle$ is the occupation probability in magnetic state $|M\rangle$ satisfying the normalization condition $\sum_M P_M = 1$, and $\Sigma(i\omega)$ is the dynamic self-energy. Following closely the procedure laid out in the second-order perturbation theory [33], the self-energy is obtained as

$$\begin{aligned} \Sigma(i\omega) = -\frac{(J_{ss}k_BT)^2}{(2\hbar v_F)^2}\sum_{MM'}\sum_{\mathbf{k},\omega_0,\omega_n}|S^+_{MM'}|^2 Tr_\sigma\big[D^0_M(\mathbf{i}\omega_0 + \mathbf{i}\omega_n) \\ \times G^0(\mathbf{k},i\omega - i\omega_0)D^0_{M'}(\mathbf{i}\omega_n)\big], \end{aligned} \quad (6)$$

where $G^0_{\sigma,\sigma'}(t,t') = -i\langle T\gamma^\dagger_{s\mathbf{k},\sigma}(t)\gamma_{s\mathbf{k},\sigma'}(t')\rangle$ is defined by unperturbed helical states and $D^0_M(t,t') = -i\langle Td^\dagger_M(t)d_M(t')\rangle$ is defined by unperturbed pseudofermions. Using Matsubara frequencies $\omega_n = (2n+1)\pi k_BT$ for fermions and $\omega_0 = 2n\pi k_BT$ for bosons, we obtain

$$\begin{aligned} \Sigma(i\omega) = \frac{J^2_{ss}}{8\pi(\hbar v_F)^2}\sum_{MM';\sigma}(|S^+_{MM'}|^2 + |S^-_{MM'}|^2)\int_0^\Lambda \varepsilon_{\mathbf{k}}d\varepsilon_{\mathbf{k}} \\ \times (P_M - P_{M'})\frac{1 + n_B(E_{M'M}) - f(\varepsilon_{\mathbf{k}\sigma})}{i\omega - \varepsilon_{\mathbf{k}\sigma} - E_{M'M}}, \end{aligned} \quad (7)$$

where Λ is a cutoff energy, $E_{M'M} = E_{M'} - E_M$, and $f(x)$ and $n_B(x)$ are the Fermi and Bose distribution functions, respectively. By replacing $i\omega \to \omega + i\eta$, the spin-resolved LDOS can be calculated by $\rho_\sigma(\mathbf{r},\omega) = \frac{-1}{2\pi}{\rm Im}[G_{\sigma\sigma}(\mathbf{r},\mathbf{r},\omega)]$.

III. DIRAC-POINT RESONANCE

We first consider the local spin and TI surface in the thermal equilibrium condition where $P_M = e^{-E_M/k_BT}/\Sigma_i e^{-E_i/k_BT}$ and $\langle S_z\rangle = 0$. In Fig. 1, we plot the evolution of electronic LDOS, $\rho = \rho_\uparrow + \rho_\downarrow$, with uniaxial anisotropy magnetic parameter D. Obviously, the impurity effect makes the LDOS deviate from Dirac linear structure (black dotted line), with its pattern depending heavily on the strength of D. For small D (e.g., $D = 0.06$), there are two strong resonance peaks located on both sides of the Dirac point ($\omega = 0$), whose positions are approximately determined by the real part ${\rm Re}[1 - V_{im}(i\omega)G^0(0,i\omega)] = 0$. The double peaks are symmetric around $\omega = 0$ due to ${\rm Im}[\Sigma(-\omega)] = {\rm Im}[\Sigma(\omega)]$. A similar

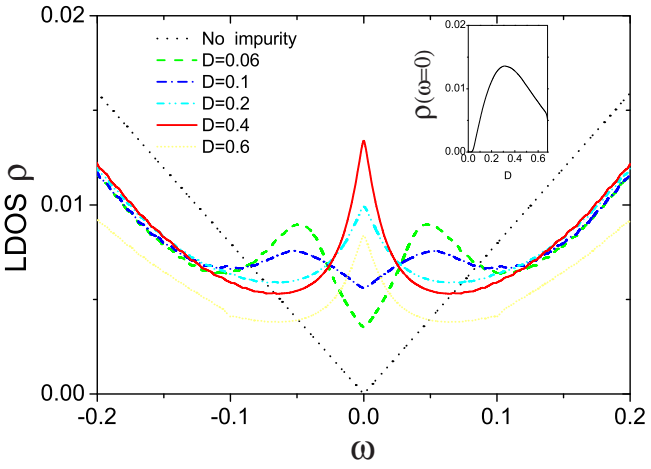

FIG. 1. (Color online) Electronic LDOS in thermal equilibrium for several values of uniaxial magnetic anisotropy D, as indicated. The black dotted line plotted for reference corresponds to the V-shape Dirac cone structure without the impurity. The other parameters are $E = 0$, $k_BT = 0.3$, $r = 6$, $S = 2$, $J_L = 0.01$, $J_R = 10$, $\Lambda = 1$, and $\mu_s = 0$ in units of $\hbar v_F$.

resonance phenomenon was reported in Refs. [9,15–17]. With increasing D, the LDOS at the Dirac point increases, accompanied with lowering and broadening of the double peaks. Interestingly, a remarkable central resonant peak develops for stronger D (e.g., $D = 0.4$) exactly at the Dirac point, whereas two side resonances shrink rapidly to double wells, heavily destroying the typical Dirac V-shape structure. With further increasing D, the DPR peak exhibits nonmonotonous dependence, as shown in the inset. The same description is suitable for the LDOS variation with in-plane magnetic parameter E.

The presented DPR behavior is quite different from that of low-energy resonances induced by strong potential impurities or phonon-assisted inelastic scattering [9,15–17]. In the latter, with increasing scattering potential the resonance peaks can be closer and closer to the Dirac point but with quickly shrinking magnitude at the same time, and in the limit of a strong impurity potential the resonances completely vanish at the Dirac point. Here, we produce either the low-energy resonances near the Dirac point or the DPR, depending on the anisotropy strength of magnetic atoms. This would be helpful to understand the observed resonance phenomena, e.g., in experiment [10] where two types of Fe atoms exhibit different resonance behaviors.

In order to clarify the origin of the DPR, we derive the analytical expression for $r \gg \hbar v_F/\Lambda$ and obtain the change of the diagonal term of the Green's function as

$$\delta G_{\sigma\sigma}(\mathbf{r},\mathbf{r},\omega) = \frac{1}{16(\hbar v_F)^2}\left[\frac{f_1^2(M_\sigma-\Sigma)}{1+g(M_\sigma-\Sigma)}+\frac{f_0^2(M_\sigma+\Sigma)}{1-g(M_\sigma+\Sigma)}\right], \quad (8)$$

where $f_0 = \omega Y_0(\frac{|\omega|r}{\hbar v_F}) - i|\omega| J_0(\frac{|\omega|r}{\hbar v_F})$ and $f_1 = \omega J_1(\frac{|\omega|r}{\hbar v_F}) + i|\omega| Y_1(\frac{|\omega|r}{\hbar v_F})$ with $g = \frac{1}{4(\hbar v_F)^2}[\frac{\omega}{\pi}\ln(\frac{\omega^2}{\Lambda^2-\omega^2}) - i|\omega|]$, $M_{\uparrow(\downarrow)} = \pm J_s\langle S_z\rangle/2$, and $J_n(x)$ and $Y_n(x)$ being the Bessel functions of the first and second kind [9,17]. At $\omega = 0$, we have $f_0^2 = 0$ and $\mathrm{Re}\,\Sigma(\omega) = 0$ so that the LDOS reduces to $\rho_\sigma(\omega = 0) = \frac{1}{2\pi}\mathrm{Re}[f_1^2]\mathrm{Im}[\Sigma(\omega)]$. Obviously, nonzero $\mathrm{Re}[f_1^2]$ and $\mathrm{Im}[\Sigma(\omega)]$ are two necessary requirements for creating the DPR. f_1 comes essentially from the spin rotation for the electron propagating on the TI surface between point $\mathbf{r}$ and the impurity site, and appears in the off-diagonal element of $G^0(\mathbf{r},\omega) = \frac{1}{4(\hbar v_F)^2}[f_0 + f_1(\sigma\cdot\hat{\theta})]$ with $\hat{\theta}$ the spatial angle of $\mathbf{r}$. The finite imaginary part of $\Sigma(\omega)$ is directly related to the fermion lifetime in spin-inelastic scattering processes with energy transfer, in which the magnetic anisotropy plays a crucial role. Moderately strong anisotropy is required to enhance the spin-inelastic transitions and then supports the DPR formation. Note that in the experiment [10] Fe atoms were shown to have considerable magnetic anisotropy, which should be the origin of the DPR.

IV. ELECTRICAL MANIPULATION OF DPR

Now we turn to the nonequilibrium effect of the quantum spin due to the spin-transfer torque. Suppose that a STM with a magnetized tip is placed above the nanomagnet, which has been extensively employed to explore the spin dynamics of high-spin nanomagnets adsorbed on metallic surfaces [34,35]. When a bias voltage is applied between the tip and surface, spin-dependent electronic transports lead to nonequilibrium occupations and then a finite magnetization $\langle S_z\rangle$. In this case, P_M of nonequilibrium spin states are governed by the dynamical master equations [36,37]:

$$\partial P_M(t)/\partial t = \sum_{\eta\eta',M'\neq M} W^{\eta\leftarrow\eta'}_{M,M'}P_{M'} - W^{\eta'\leftarrow\eta}_{M',M}P_M. \quad (9)$$

Here $W^{\eta'\leftarrow\eta}_{M',M}$ is the transition rate of transport electrons going from lead η to η' with $\eta = t\ (s)$ standing for the tip (surface), accompanied with spin flip of the magnetic impurity via spin excitation $S^+_{M',M}$ and spin disexcitation $S^-_{M',M}$. Taking the tip-surface Hamiltonian to be $H^{\mathrm{ex}}_{ts} = \sum_{\mathbf{k}\mathbf{k}'}\frac{J_{ts}}{2}c^\dagger_{s\mathbf{k}}\sigma\cdot\mathbf{S}c_{t\mathbf{k}'} + \mathrm{H.c.}$ with $c_{t\mathbf{k}}$ the annihilation operator for tip electrons, one can derive from Fermi's golden rule

$$W^{\eta'\leftarrow\eta}_{M',M} = \frac{\pi}{2\hbar}J^2_{\eta\eta'}[|S^+_{M',M}|^2D^t_\uparrow + |S^-_{M',M}|^2D^t_\downarrow] \times\int_{-\Lambda}^{\Lambda} f(\varepsilon - E_{MM'} + \mu_{\eta'} - \mu_\eta)f^-(\varepsilon)\rho_0(\varepsilon)d\varepsilon, \quad (10)$$

where $\rho_0(\varepsilon) = \frac{|\varepsilon|}{4\pi(\hbar V_F)^2}$, $f^-(\varepsilon) = 1 - f(\varepsilon)$, D^t_σ is the σ-spin DOS of the tip electrons, and μ_η is the chemical potential of terminal η. Obviously, the bias dependence of the transition rate provides a route to electrically control P_M and in turn the self-energy in Eq. (7).

The spin polarization of the magnetic tip is defined as $\chi^t = (D^t_\uparrow - D^t_\downarrow)/D^t_0$ with $D^t_0 = D^t_\uparrow + D^t_\downarrow$. We plot the spin-dependent LDOS ρ_σ for lower- and higher-temperature regimes, respectively, in Figs. 2(a) and 2(b), where the black lines with overlapping $\rho_\uparrow$ and $\rho_\downarrow$ correspond to the $\chi^t = 0$ case of the nonmagnetic tip. At lower temperatures (i.e., $k_BT = 0.01$), as shown in Fig. 2(a), a finite spin polarization (e.g., $\chi^t = 0.6$) lifts the spin degeneration of the double side resonances by generating nonzero $\langle S_z\rangle$. One resonance peak is enhanced and the other is suppressed, whereas the LDOS close to the Dirac point remains unchanged. In this case, the bias-driven nanomagnet behaves only like a classic magnet [9]. Changing the bias parity merely causes the two spin species to switch roles.

With the increase of temperature (i.e., $k_BT = 0.3$), a most interesting result is shown in Fig. 2(b), where the initially weak DPR for $\chi^t = 0$ becomes quite sharp when the STM tip is polarized with $\chi^t = 0.6$ and its height further increases with polarization χ^t. This scenario also can be manipulated with a bias voltage applied between the STM tip and TI surface. As shown in the inset, with increasing the bias voltage, no matter whether it is positive or negative, the DPR peak quickly rises and then tends to be saturated. This provides a good way to electrically tune the LDOS of the Dirac point, and even to engineer the Dirac cone. The underlying physical mechanism is that in the spin-polarized transport processes the spin-flip transitions can lead to a redistribution of occupations among magnetic states $|M\rangle$, as depicted in Fig. 2(c). As pointed out above, the occupations P_M at $V_{\mathrm{bias}} = 0$ obey the thermal equilibrium statistics, regardless of the value of χ^t. However, a finite bias redistributes the occupation, and importantly during this process the difference of occupations between adjacent

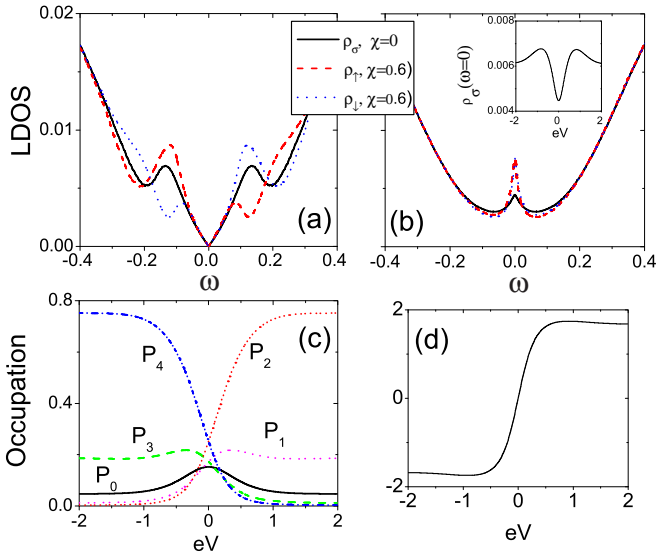

FIG. 2. (Color online) Spin-resolved LDOS ρ_σ in the spin nonequilibrium case due to spin-dependent electron tunneling between the STM tip of $\chi^t = 0.6$ and TI surface via nanomagnet for $k_BT = 0.01$ (a) and $k_BT = 0.3$ (b), with $eV_{\rm bias} = 2$, $D = 0.2$, and $E = 0.01$. Here, the black solid lines with identical $\rho_\uparrow$ and $\rho_\downarrow$ correspond to the nonmagnetic case. The dependence on the bias voltage of dynamic evolution of occupation P_M (c), net magnetization of the nanomagnet (d), and height of the zero-energy resonant peak (inset) are plotted from (b). The other parameters are the same as in Fig. 1.

levels, e.g., $P_2 - P_1$ in Fig. 2 (c), increases, which significantly modifies the self-energy $\Sigma(\omega)$ in Eq. (7). At the same time, the nanomagnet is polarized as shown in Fig. 2(d). Even so, the DPRs of the two spin species are almost identical, as can be seen from Eq. (8), where $\delta G_{\sigma\sigma}(\mathbf{r},\mathbf{r},\omega)$ is independent of M_σ at $\omega = 0$.

V. FRIEDEL OSCILLATIONS OF DPR PEAK

The height of the DPR peak is strongly dependent on the spatial distance r measured from the impurity position. The LDOS at $\omega = 0$ is plotted as a function of r in Fig. 3(a). Obviously, the typical pattern of Friedel oscillations is presented due to the interference of incoming and outgoing waves around the local magnetic moment. At the impurity position ($r = 0$), the DPR is completely suppressed. We wish to point out that the present Friedel oscillations at $\omega = 0$ are distinguished from those in the Kondo regime [22], where the Friedel oscillations decay as an inverse-square $1/r^2$ law. In Fig. 3(b), $r^2\rho(\omega = 0)$ is plotted as a function of r. It is found that the Friedel oscillations do not decay as a simple $1/r^2$ law,

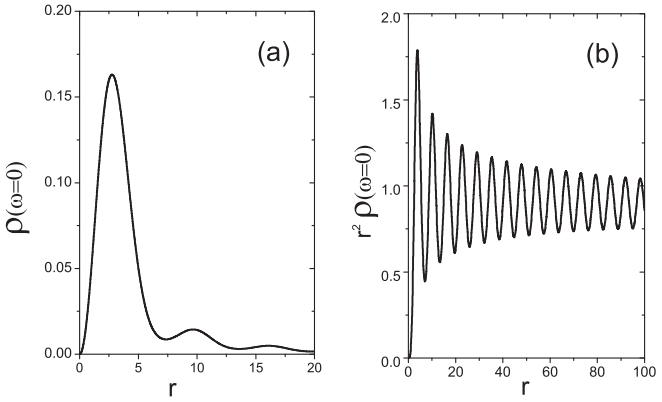

FIG. 3. Friedel oscillations at the Dirac point for $\rho(\omega = 0)$ (a) and $r^2\rho(\omega = 0)$ (b) with r. Here $D = 0.05$, $E = 0.01$, $\chi^t = 0.6$, $eV_{\rm bias} = 2$, $\mu_s = 0.5$, and the other parameters are the same as in Fig. 1.

but approximately obey $e^{-\lambda r/\hbar v_F}/r^2$ with an additional relaxation factor of $\lambda \approx 0.03$ for parameters chosen here.

VI. SUMMARY

We study the scattering of Dirac electrons off a high-spin nanomagnet with magnetic anisotropy adsorbed on a TI surface, similar to the setup in the experiment [10]. Beyond the classic spin model, the spin-inelastic processes involving transitions between its internal magnetic levels are taken into account. It is found that the spin-inelastic scattering can create a LDOS resonance peak exactly at the Dirac point, locally destroying the topologically protected Dirac surface-state spectrum at the Dirac point, quite different from previously reported resonances created by strong impurity potential or local bosons [9,15–17], where the Dirac point is never destroyed. The result is attributed to the joint effect of the spin rotation of the electron propagating on the TI surface and the inelastic-scattering induced imaginary part of the self-energy, where the magnetic anisotropy of the nanomagnet plays a crucial role. We further propose an approach to tune electrically the DPR by using a spin-polarized scanning tunneling microscopy. Experimentally, this is important since it can facilitate the observation of DPR even for impurities with weak magnetic anisotropy.

ACKNOWLEDGMENTS

This work was supported by the State Key program for Basic Research of China (Grant No. 2010CB923400), by the National Natural Science Foundation of China (Grants No. 11174088, No. 11474106, No. 11225420, 11274124, and No. 11174125), and by PCSIRT in China (Grant No. IRT1243).

[1] X. L. Qi and S. C. Zhang, Rev. Mod. Phys. **83**, 1057 (2011).
[2] P. Roushan, J. Seo, C. V. Parker, Y. S. Hor, D. Hsieh, D. Qian, A. Richardella, M. Z. Hasan, R. J. Cava, and A. Yazdani, Nature (London) **460**, 1106 (2009).
[3] D. Soriano, F. Ortmann, and S. Roche, Phys. Rev. Lett. **109**, 266805 (2012).
[4] Q. Liu, C. X. Liu, C. Xu, X. L. Qi, and S. C. Zhang, Phys. Rev. Lett. **102**, 156603 (2009).

[5] Y. L. Chen, J. H. Chu, J. G. Analytis, Z. K. Liu, K. Igarashi, H. H. Kuo, X. L. Qi, S. K. Mo, R. G. Moore, D. H. Lu, M. Hashimoto, T. Sasagawa, S. C. Zhang, I. R. Fisher, Z. Hussain, and Z. X. Shen, Science **329**, 659 (2010).

[6] S. Y. Xu, M. Neupane, C. Liu, D. Zhang, A. Richardella, L. Andrew Wray, N. Alidoust, M. Leandersson, T. Balasubramanian, J. Sanchez-Barriga *et al.*, Nat. Phys. **8**, 616 (2012).

[7] M. R. Mahani, A. Pertsova, M. F. Islam, and C. M. Canali, Phys. Rev. B **90**, 195441 (2014).

[8] L. A. Wray, S. Y. Xu, Y. Xia, D. Hsieh, A. V. Fedorov, Y. S. Hor, R. J. Cava, A. Bansil, H. Lin, and M. Z. Hasan, Nat. Phys. **7**, 32 (2011).

[9] R. R. Biswas and A. V. Balatsky, Phys. Rev. B **81**, 233405 (2010).

[10] J. Honolka, A. A. Khajetoorians, V. Sessi, T. O. Wehling, S. Stepanow, J. L. Mi, B. B. Iversen, T. Schlenk, J. Wiebe, N. B. Brookes, A. I. Lichtenstein, Ph. Hofmann, K. Kern, and R. Wiesendanger, Phys. Rev. Lett. **108**, 256811 (2012).

[11] M. R. Scholz, J. Sánchez-Barriga, D. Marchenko, A. Varykhalov, A. Volykhov, L. V. Yashina, and O. Rader, Phys. Rev. Lett. **108**, 256810 (2012).

[12] T. Schlenk, M. Bianchi, M. Koleini, A. Eich, O. Pietzsch, T. O. Wehling, T. Frauenheim, A. Balatsky, J. L. Mi, B. B. Iversen, J. Wiebe, A. A. Khajetoorians, Ph. Hofmann, and R. Wiesendanger, Phys. Rev. Lett. **110**, 126804 (2013).

[13] T. Valla, Z. H. Pan, D. Gardner, Y. S. Lee, and S. Chu, Phys. Rev. Lett. **108**, 117601 (2012).

[14] J. Henk, A. Ernst, S. V. Eremeev, E. V. Chulkov, I. V. Maznichenko, and I. Mertig, Phys. Rev. Lett. **108**, 206801 (2012).

[15] Z. Alpichshev, R. R. Biswas, A. V. Balatsky, J. G. Analytis, J. H. Chu, I. R. Fisher, and A. Kapitulnik, Phys. Rev. Lett. **108**, 206402 (2012).

[16] A. M. Black-Schaffer and A. V. Balatsky, Phys. Rev. B **85**, 121103(R) (2012).

[17] J. H. She, J. Fransson, A. R. Bishop, and A. V. Balatsky, Phys. Rev. Lett. **110**, 026802 (2013).

[18] R. Žitko, Phys. Rev. B **81**, 241414(R) (2010).

[19] H. F. Lü, H. Z. Lu, S. Q. Shen, and T. K. Ng, Phys. Rev. B **87**, 195122 (2013).

[20] I. Kuzmenko, Y. Avishai, and T. K. Ng, Phys. Rev. B **89**, 035125 (2014).

[21] A. K. Mitchell, D. Schuricht, M. Vojta, and L. Fritz, Phys. Rev. B **87**, 075430 (2013).

[22] M. T. Tran and K. S. Kim, Phys. Rev. B **82**, 155142 (2010).

[23] M. V. Costache, I. Neumann, J. F. Sierra, V. Marinova, M. M. Gospodinov, S. Roche, and S. O. Valenzuela, Phys. Rev. Lett. **112**, 086601 (2014).

[24] H. Gawronski, J. Fransson, and K. Morgenstern, Nano Lett. **11**, 2720 (2011).

[25] A. Hurley, A. Narayan, and S. Sanvito, Phys. Rev. B **87**, 245410 (2013).

[26] J. C. Oberg, M. R. Calvo, F. Delgado, M. Moro-Lagares, D. Serrate, D. Jacob, J. Fernandez-Rossier, and C. F. Hirjibehedin, Nat. Nanotech. **9**, 64 (2014).

[27] R. Q. Wang, R. Shen, S. L. Zhu, B. G. Wang, and D. Y. Xing, Phys. Rev. B **85**, 165432 (2012).

[28] F. Delgado, J. J. Palacios, and J. Fernández-Rossier, Phys. Rev. Lett. **104**, 026601 (2010).

[29] R. Q. Wang, L. Sheng, R. Shen, B. G. Wang, and D. Y. Xing, Phys. Rev. Lett. **105**, 057202 (2010).

[30] A. Hurley, N. Baadji, and S. Sanvito, Phys. Rev. B **84**, 035427 (2011).

[31] P. Thalmeier and A. Akbari, Phys. Rev. B **86**, 245426 (2012).

[32] D. A. Abanin and D. A. Pesin, Phys. Rev. Lett. **106**, 136802 (2011).

[33] G. D. Mahan, *Many-Particle Physics*, 2nd ed. (Plenum, New York, 1990).

[34] S. Krause, L. Berbil-Bautista, G. Herzog, M. Bode, and R. Wiesendanger, Science **317**, 1537 (2007).

[35] S. Loth, K. von Bergmann, M. Ternes, A. F. Otte, C. P. Lutz, and A. J. Heinrich, Nat. Phys. **6**, 340 (2010).

[36] C. Timm and F. Elste, Phys. Rev. B **73**, 235304 (2006).

[37] H. Z. Lu, B. Zhou, and S. Q. Shen, Phys. Rev. B **79**, 174419 (2009).